The Impact of System Configuration on Device Radiation Damage Testing of Optical Components

S.D. Kniffin,[1] R.A. Reed,[2] P.W. Marshall,[3] J.W. Howard,[4] H.S. Kim[4], and J.P. Schepis[2]

1. NASA/Orbital Sciences Corporation, Dulles, VA 20166
2. NASA/Goddard Space Flight Center, Greenbelt, MD 20771
3. Consultant, Brookneal, VA 24528
4. NASA/Jackson and Tull, Washington, D.C. 20018

ABSTRACT:

We report on the significant impact that system configuration had on the radiation damage testing of a light emitting diode-phototransistor pair for the Hubble Space Telescope Wide Field/Planetary Camera 2.

INTRODUCTION

In this paper, we present an example of an in-flight anomaly that illustrates that generic radiation test methods may yield misleading results when applied to specific system configurations. In this case, a Texas Instruments (TI) TIL25 P-N GaAs light-emitting diode (LED) and a TIL601 N-P-N planar silicon phototransistor (PT) pair were used as an optical encoder pair for operation of the instrument shutters in the Wide Field/Planetary Camera 2 (WF/PC 2) shutters aboard the Hubble Space Telescope (HST). The pair was operated in a manner consistent with prior flight experience using LED-PT pairs and was radiation tested as a pair prior to flight. However, in the application, the ability of this pair to generate a proper signal was impaired by the system configuration. This configuration reduced the operating margin below that expected from radiation-induced degradation, resulting in failure of the encoder.

HST's orbit of 28.5° at 598km results in a proton dominated radiation environment. Protons cause displacement damage (as well as total ionizing dose (TID) degradation) in susceptible electronic devices. This is particularly true in optoelectronic devices [1-12]. In LEDs, this displacement damage creates charge recombination centers that diminish the devices' light out put. In PT's, the protons degrade performance by means of TID damage as well as displacement damage. The damage results in parametric degradation of the device, including an increase in rise time to a given optical signal.

THE ANOMALY

In the summer and fall of 2000, two on-orbit anomalies occurred in the WF/PC 2 shutter assembly in the 7th year of a planned 5-year mission [13]. The anomaly caused the instrument to go into safe mode (power down and await ground command). The encoders that determine if the shutter blades are in the closed or open positions were erroneously reporting that both shutters were closed. This is an impossible condition since it means the shutter vanes would have to occupy the same physical location. The encoder determined that the shutter was closed when the light from the LED did not turn on the PT through an aperture in the blade of the shutter assembly within a preprogrammed time interval. The resultant "off" current in the PT was read through a CMOS gate into the WF/PC 2 microprocessor after a preset time. If there is low current at that time, then the shutter is closed and the circuit then switches off.

An Anomaly Review Board (ARB) was convened to determine the cause of the anomaly. The ARB failure tree included 12 possible failure mechanisms, 8 mechanical and 4 electrical. Telemetry excluded the 8 mechanical and 2 of the electrical mechanisms. The only remaining credible failure mechanisms were degraded performance of the LED and/or the PT, with radiation being the most likely cause. Because of the LED – PT pair's long flight history and its prior radiation characterization, radiation effects experts were not invited to the first series of meetings of the ARB. However, gradually it began to appear that the WF/PC 2 application was sufficiently different from previous missions, that further characterization was warranted.

In the WF/PC 2 application, light from the LED had to shine through a 20mil diameter hole, through a 20mil wide slot in the encoder blade and through another 20mil diameter hole to reach the PT. Goddard Space

Flight Center carried out additional radiation testing of the LED-PT pair that reflected these differences.

This testing determined that with these apertures in place, radiation-induced damage in the LED – PT pair significantly increased the rise time of the PT, resulting in the PT being sampled by the microprocessor before the PT current was saturated. Without the restriction of the aperture, which resulted in significantly less light reaching the PT. For this case, it was the combined effect of application configuration and minor device degradation that caused the anomaly.

OPERATIONAL THEORY AND DEVICE DESCRIPTION

A simple schematic of the use of a LED-PT pair is shown in Fig. 1.

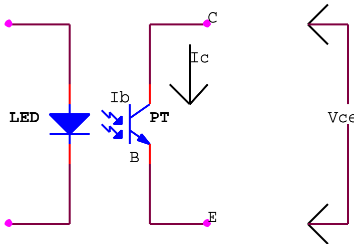

Figure 1: Schematic of LED-PT pair with voltages and currents defined.

The forward current in the LED gives rise to the base current (I_B) of the PT, which is simply the photocurrent generated by the incident light from the LED. As illustrated by the Gummel plot in Fig. 2, the PT collector current (I_C) is strongly dependent on I_B for most given collector-emitter voltages (V_{CE}) (Line A). It is common practice to choose an LED and PT that generates the desired I_C with the minimum V_{CE} (Line B). This makes I_C relatively stable even if there are small changes in I_B. Thus if there is degradation in the LED, it should not affect the operation of the pair. However, even this technique may be vulnerable if the degradation is severe or if there is some aspect of a system configuration that affects I_B.

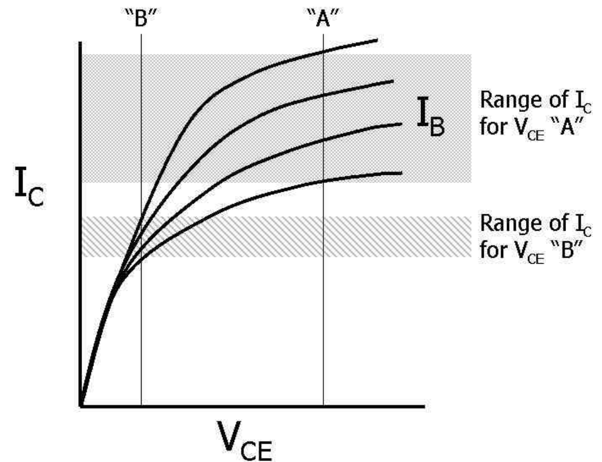

Fig. 2: Gummel Plot for reference showing a region "A" with a significant margin for functional I_B values and a region "B" with severely limited margin. [14]

EXPERIMENT

Device pairs from the flight lot were exposed to 63MeV protons with a test flux of 1.7×10^8 protons/cm^2/s at the University of California at Davis Crocker Nuclear Laboratory [15]. The PT current, voltage, circuit bias, and rise time characteristics of the pair were monitored for radiation-induced degradation at various fluence levels with and without an aperture to determine the overall affect of the aperture on the application on orbit. Figure 3 shows the bias conditions for the devices as tested.

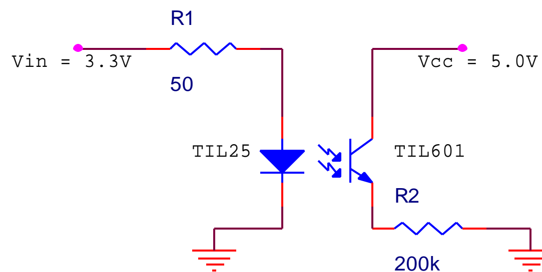

Fig. 3: Schematic of LED/PT test bias conditions.

The input to the TIL25 LED was a 110ms, 3.3V pulse that resulted in approximately 40mA forward current through the LED. In order to characterize the results for the HST WFC2 application, the voltage across resistor R2, collector current, and the rise time of the TIL601 in response to this pulse were measured.

LED-PT pair #1 had a TIL25 and TIL601 mounted on the test board approximately 170mils apart with only air between the two devices. All measurements were taken in this configuration. The testing sequence involved taking initial measurements of PT current, circuit bias, and rise time, followed by step-wise irradiation of the LED-PT pair, and a repetition of the parametric measurements until the devices exhibited significant degradation.

LED-PT pair #2 was mounted to the board in the same way, with the majority of the data taken with a 150mil wide structure between the LED and phototransistor. The structure had a 20mil diameter aperture through it, aligned such that light from the LED could reach the active region of the phototransistor. Prior to irradiation, initial measurements were made on LED-PT pair #2 with the structure removed (the same as the measurements made on LED-PT #1). Next, the initial measurements were repeated with the structure in place under the same test conditions. The unit was irradiated and tested in steps as in LED-PT #1 but with the structure left in place. After the final exposure, measurements with and finally without the structure were made. It should be noted that the aperture was manually placed between the TIL25 and TIL601 and was not an exact copy of the flight configuration. The results indicated that the uncertainty caused by this difference was not significant. When the HST project implemented the corrective action, it was sufficiently conservative to overwhelm any uncertainties in the measurements taken.

RESULTS AND DISCUSSION

Measurements of the rising edge of the voltage pulse across R2 were taken from the oscilloscope for LED-PT pair #1 and pair #2 with and without the 20mil aperture for various exposure levels. Figure 4 shows a comparison of the results between LED-PT pair #1 and LED-PT pair #2 (without and with the 20mil aperture). All figures are normalized to time = 0sec at the point where the input pulse was introduced to the LED. As can be seen from the graphs, the rise time for the phototransistor increases from ~20µs to over 400µs with increasing proton fluence. The length of the rise time may critically affect the functionality of the LED-PT pair in this application, since the microprocessor samples the PT state at a fixed time after the LED is turned on. The fact that LED-PT pair #2 behaves identically to LED-PT pair #1 in the absence of the aperture indicates that it is the presence of the aperture in the application that is responsible for the observed discrepancy between on-orbit performance and the original radiation test results. The dark bar at 32µs indicates the time at which the microprocessor sampled the PT after the LED was turned on.

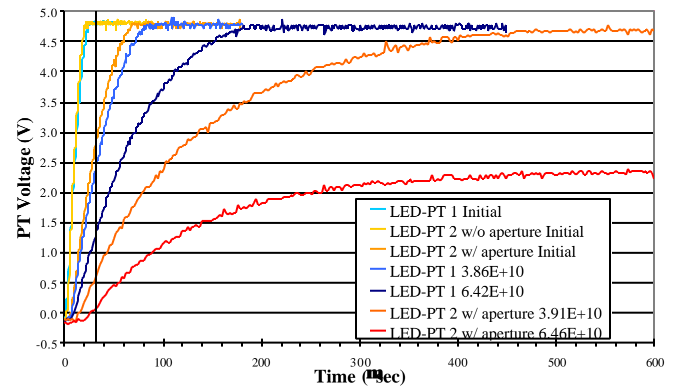

Fig. 4: Comparison of the effect of the 20mil aperture on the test results between devices. Fluences are in p/cm^2. The black bar at 32µs represents the time at which the processor samples the PT.

Figure 5 shows the data for the PT collector current as a function of the proton exposure for both LED-PT pairs and both configurations for LED-PT pair #2. It is plotted as I/I_0. It is important to note that the results for LED-PT pair #2 without the aperture (yellow filled diamond) fall on the same curve as LED-PT pair #1 (empty blue diamond) that had no aperture. There is little degradation until approximately 5x10^{10}p/cm^2. At this point the aperture begins to make a dramatic difference. LED-PT pair #1 and #2 without an aperture continue with only somewhat increased degradation until 1x10^{11}p/cm^2, whereas LED-PT pair #2 with the aperture exhibits significant degradation, falling to approximately 20% of its initial value by 1x10^{11}p/cm^2. These results are attributable to the decreased I_C resulting from a decrease in I_B as demonstrated in Fig. 2.

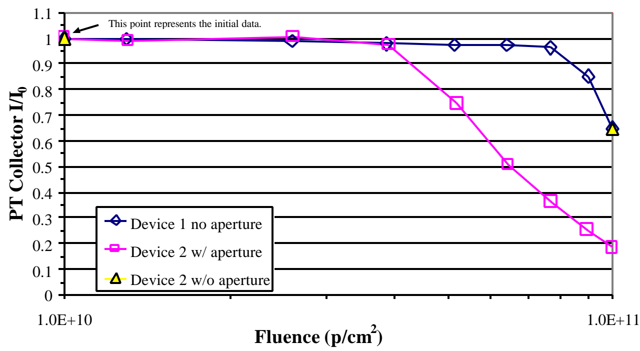

Fig. 5: Photodiode collector current as a function of the proton fluence.

The third parameter of interest was the saturation voltage that was seen across the resistor (R2) on the output of the phototransistor. This is the maximum voltage across R2 in response to the LED input pulse. There is little degradation until 5×10^{10}p/cm^2 where similar results occurred with and without the aperture. The peak voltage is down to 75% of its initial value for LED-PT pair #1 and approximately 15% for the LED-PT pair #2 by 1×10^{11}p/cm^2. Again, LED-PT pair #1 and LED-PT pair #2 performed similarly when LED-PT pair #2 was measured without the aperture structure.

Table 1 presents the radiation test data at the critical fluences for the mission after 7 years. Table 2 presents the radiation test data at the critical fluences for the mission after 10 years. The proton fluences were predicted by the AP8 model in CREME96. The predicted 7-year mission fluence is 2.1×10^{10} p/cm^2 and the predicted 10-year mission fluence is 3.2×10^{10} p/cm^2 with 2x uncertainty [16]. For the data presented in Table 1, Time = 0µsec is defined as the initiation of the pulse in the LED. The proton fluences steps did not exactly match the margins and are given below the mission fluence heading.

	1.1×10^{10} p/cm^2 (min.)	2.1×10^{10} p/cm^2 (predicted)	4.2×10^{10} p/cm^2 (max.)
Closest Test Fluence (63MeV p+)	1.3×10^{10} p/cm^2	2.6×10^{10} p/cm^2	3.9×10^{10} p/cm^2
PT I/I_O	0.99	1.0	0.97
PT V_{MAX}	4.8V	4.8V	4.8V
PT V at 32µs	1.6V	1.0V	0.6V
PT V at 100µs	4.4V	3.2V	2.4V
PT V at 300µs	----	4.7V	4.2V
PT V at 500µs	----	4.8V	4.7V

Table 1: Parametric values at critical fluences after 7 years on orbit.

	1.6×10^{10} p/cm^2 (min.)	3.2×10^{10} p/cm^2 (predicted)	6.4×10^{10} p/cm^2 (max.)
Closest Test Fluence (63MeV p+)	1.3×10^{10} p/cm^2	3.9×10^{10} p/cm^2	6.5×10^{10} p/cm^2
PT I/I_O	0.99	0.97	0.51
PT V_{MAX}	4.8V	4.8V	2.4V
PT V at 32µs	1.6V	0.6V	0.1V
PT V at 100µs	4.4V	2.4V	1.2V
PT V at 300µs	----	4.2V	2.1V
PT V at 500µs	----	4.7V	2.3V

Table 2: Parametric values at critical fluences after 10 years on orbit.

ANOMALY RESOLUTION

In order to counter the effects of the increased rise time in the PT, a RAM patch was sent to the WF/PC 2 microprocessor to change the sampling time from the original 32µs to 10ms. Following this corrective patch, no further anomalies have been reported to date.

LESSONS LEARNED

Because system configuration can strongly affect the validity of test results, test procedures and setups must be designed with adequate fidelity to the application—even if this compromises somewhat the generality of the test procedure. The very versatility of optoelectronic devices makes them particularly susceptible to application-specific anomalies. Close communication between the project and the test engineers is essential at all stages of the design process—from device selection, through performance verification (including radiation testing) and construction—to ensure that the test is truly valid for the application. More simply, you must not only fly what you test and test what you fly, you must also test the way you fly.

REFERENCES

[1] K.A. LaBel, et al. "Proton-Induced Transients in Optocouplers: In-Flight Anomalies, Ground Irradiation Test, Mitigation and Implications." *IEEE Trans. Nuc. Sci.* 44(6), December 1997: 1885-1892.
[2] R.A. Reed, et al. "Emerging Optocoupler Issues with Energetic Particle-Induced Transients and Permanent Radiation Degradation." *IEEE Trans. Nuc. Sci.*, 45(6), December 1998: 2833-2841.
[3] K.A. LaBel, et. al., "A Compendium of Recent Optocoupler Radiation Test Data", *IEEE Radiation Effects Data Workshop*, July 2000: 123-124.
[4] R.A. Reed, et al. "Energy Dependence of Proton Damage in AlGaAs Light-Emitting Diodes." *IEEE Trans. Nuc. Sci.*, 47(6), December 2000: 2492-2499.

[5] M.V. O'Bryan, et al. "Single Event Effect and Radiation Damage Results for Candidate Spacecraft Electronics." *IEEE Radiation Effects Data Workshop*, July 1998: 39-50.
[6] M.V. O'Bryan, et al. "Recent Radiation Damage and Single Event Effect Results for Microelectronics." *IEEE Radiation Effects Data Workshop*, July 1999: 1-14.
[7] M. D'Ordine. "Proton Displacement Damage in Optocouplers." *IEEE Radiation Effects Data Workshop*, July 1997: 122-124.
[8] C.E. Barnes, et al. "Radiation Effects in Optoelectronic Devices." Sandia Report, SAND84-0771, 1994.
[9] A.H. Johnston, et al. "Proton Degradation of Light-Emitting Diodes." *IEEE Trans. Nuc. Sci.,* 46(6), December 1999: 1781-1789.
[10] B.G, Rax, et al. "Total Dose and Proton Damage in Optocouplers." *IEEE Trans. Nuc. Sci.,* 43(6), December 1996: 3167-3173.
[11] A.H. Johnston, et al. "Single-Event Upset Effects in Optocouplers." *IEEE Trans. Nuc. Sci.,* 45(6), December 1998: 2867-2875.
[12] A.H. Johnston, et al. "Angular and Energy Dependence of Proton Upset in Optocouplers." *IEEE Trans. Nuc. Sci.,* 46(6), December 1999: 1335-1341.
[13] J.P. Schepis, private communication.
[14] S.M. Sze, Semiconductor Devices: Physics and Technology, 2nd ed. Based on Fig.10 p.145, 2002.
[15] S.D. Kniffin, et. al., "Proton Displacement Testing of the TIL25 and TIL601 as Configured in HST WFC2,"
http://radhome.gsfc.nasa.gov/top.htm
[16] J.L. Barth and M. Xapsos, private communication.